Published OnlineFirst November 7, 2012; DOI: 10.1158/1078-0432.CCR-12-1099

Imaging, Diagnosis, Prognosis

Clinical Cancer Research

Identification of Serum Proton NMR Metabolomic Fingerprints Associated with Hepatocellular Carcinoma in Patients with Alcoholic Cirrhosis

Pierre Nahon[1,4], Roland Amathieu[5,6], Mohamed N. Triba[5], Nadia Bouchemal[5], Jean-Charles Nault[1], Marianne Ziol[2], Olivier Seror[3], Gilles Dhonneur[6], Jean-Claude Trinchet[1], Michel Beaugrand[1], and Laurence Le Moyec[7]

Abstract

Purpose: Metabolomics depicts metabolic changes in biologic systems using a multiparametric analysis technique. This study assessed the metabolomic profiles of serum, obtained by proton nuclear magnetic resonance (NMR) spectroscopy, from cirrhotic patients with and without hepatocellular carcinoma (HCC).

Experimental Design: The study included 154 consecutive patients with compensated biopsy-proven alcoholic cirrhosis. Among these, 93 had cirrhosis without HCC, 28 had biopsy-proven HCC within the Milan criteria and were eligible for curative treatment (small HCC), and 33 had HCC outside the Milan criteria (large HCC). Proton spectra were acquired at 500 MHz. An orthogonal partial latent structure [orthogonal projection to latent structure (OPLS)] analysis model was built to discriminate large HCC spectra from cirrhotic spectra. Small HCC spectra were secondarily projected using previously built OPLS discriminant components.

Results: The OPLS model showed discrimination between cirrhotic and large HCC spectra. Metabolites that significantly increased with large HCC were glutamate, acetate, and N-acetyl glycoproteins, whereas metabolites that correlated with cirrhosis were lipids and glutamine. Projection of small HCC samples into the OPLS model showed a heterogeneous distribution between large HCC and cirrhotic samples. Small HCC patients with metabolomic profile similar to those of large HCC group had higher incidences of recurrence or death during follow-up.

Conclusions: Serum NMR-based metabolomics identified metabolic fingerprints that could be specific to large HCC in cirrhotic livers. From a metabolomic standpoint, some patients with small HCC, who are eligible for curative treatments, seem to behave as patients with advanced cancerous disease. It would be useful to further prospectively investigate these patients to define a subgroup with a worse prognosis. *Clin Cancer Res; 18(24); 6714–22. ©2012 AACR.*

Introduction

Staging systems of hepatocellular carcinoma (HCC) aim to assess prognosis and to select adequate treatments for each case, particularly in patients eligible for curative procedures, such as hepatic resection, percutaneous ablation, or liver transplantation (1). However, there is still a need for biologic markers to be associated with clinical outcomes or treatment responses. A definition of the molecular classification of HCC is still preliminary and, unlike other tumors, as yet, no molecular data have been incorporated into algorithms for the routine management of liver cancer (2). A wide spectrum of serum biomarkers has been studied as potential diagnosis or prognosis tools in this setting, but their ability to refine HCC classification or to predict the patient's outcome is still debated. Consequently, the main prognostic factors used in practice are restricted to clinical features such as tumor status and liver-function impairment linked to the underlying liver disease.

Metabolomics is an "omics" technique that is situated downstream of genomics, transcriptomics, and proteomics (3). Proton nuclear magnetic resonance (^{1}H NMR) spectroscopy–based metabolomics can identify and quantify metabolic changes within a biologic system and has been applied to various pathologic conditions (4). The development of

Authors' Affiliations: [1]Service d'Hépatologie et Université Paris 13, [2]Service d'Anatomopathologie et Université Paris 13, and [3]Service de Radiologie et Université Paris 13, Hôpital Jean Verdier, AP-HP, Bondy; [4]INSERM U773, CRB3, Université Paris 7, Paris; [5]Laboratoire CSPBAT, UMR 7244, Université Paris 13, Bobigny; [6]Service d'Anesthésie-Réanimation et Université Paris 12, Hôpital Henri Mondor, AH-HP, Créteil; and [7]INSERM U902, UBIAE, Université d'Evry, Evry, France.

Note: Supplementary data for this article are available at Clinical Cancer Research Online (http://clincancerres.aacrjournals.org/).

P. Nahon and R. Amathieu contributed equally to this work.

Corresponding Author: Pierre Nahon, Service d'Hépatologie, Hôpital Jean Verdier, 93140 Bondy, France. Phone: 33-1-48-02-62-80; Fax: 33-1-48-02-62-02; E-mail: pierre.nahon@jvr.aphp.fr

doi: 10.1158/1078-0432.CCR-12-1099

Published OnlineFirst November 7, 2012; DOI: 10.1158/1078-0432.CCR-12-1099

Translational Relevance

Hepatocellular carcinoma (HCC) is one of the leading cancers worldwide in terms of incidence and mortality. Most of HCC arise on cirrhosis in western countries, alcohol intake being the main cause of cirrhosis and related HCC in these countries. The difficulties to assess the outcome of such patients stress the need to identify new biomarkers to refine the identification of those with a poorer therapeutic response. The present data enabled us to observe changes in serum metabolomic profiles in patients with advanced HCC that reflected the distinct activation or impairment of multiple biologic pathways. Furthermore, the analysis of patients with small HCC eligible for curative procedures revealed various metabolomic profiles that probably reflect differences in outcome after tumor ablation. By providing new patterns of recognition, serum metabolomic profiling may represent a clinical breakthrough to refine prognosis and to guide therapeutic procedures for these patients.

metabolomics in the field of oncology may be used to identify fingerprints, profiles, or signatures, which could be useful for screening or diagnosis procedures as well as refining prognosis or therapeutic response in various tumors, such as prostate, breast, ovarian, or brain cancers (5, 6).

Recent studies have attempted to describe the metabolic phenotype of liver cancer in heterogeneous populations of patients with HCC using ^{1}H NMR or mass spectroscopy. This has led to the identification of various metabolically impaired pathways in serum and urine (7–10). However, these data were obtained in small sample-sized cohorts of patients and important clinical information was lacking, such as the stage of liver cancer and the cause and degree of severity of the underlying liver disease, which can induce specific and serious serum metabolic disturbances (11). Furthermore, these studies were mostly restricted to Asian populations in whom cases of HCC were as a whole related to hepatitis C virus (HCV) or hepatitis B (HBV) chronic infections.

The aim of the present study was to assess serum metabolomic profiles in a large cohort of well-characterized Caucasian patients with HCC that developed in alcoholic cirrhotic liver and classified according to their tumor status.

Patients and Methods

Patients and collection of serum samples

We considered all out-patients who were consecutively referred to our Hepatology unit for the management of cirrhosis and/or HCC between January 2009 and December 2010, and who fulfilled the following inclusion criteria: (i) biopsy-proven cirrhosis and chronic daily alcohol consumption of more than 50 g; (ii) no infection from the human immunodeficiency, hepatitis B or C viruses; (iii) compensated liver disease (Child–Pugh score <8); (iv) residence in France and of Caucasian origin; and (v) availability of frozen serum samples. Exclusion criteria were: (i) treatment of HCC before serum collection; (ii) past history or on-going extrahepatic neoplasm or inflammatory systemic disease; (iii) recent history of acute or chronic liver failure in the previous 6 months.

For each patient, the date of inclusion was the date of serum collection. Demographic, clinical, and routine biologic data were recorded at inclusion. Blood samples were drawn under fasting conditions before therapeutic management of HCC. Sera were separated and stored at −80°C until analysis. All patients gave their written consent for blood sampling. The local ethics committee approved the protocol.

HCC was diagnosed according to the Barcelona criteria (12): histologic evidence or convergent demonstration of a focal lesion more than 2 cm in size and arterial hypervascularization as assessed by 2 different imaging techniques, or the combination of 1 imaging technique that showed this morphologic aspect plus an α-fetoprotein (AFP) level of 400 ng/mL or more in patients with biopsy-proven cirrhosis.

Patients were classified according to the presence and status of HCC as follows.

1. Cirrhosis group: patients with cirrhosis without evidence of HCC at the time of inclusion, as judged by negative ultrasonographic findings, serum AFP of less than 50 ng/mL. All patients were prospectively evaluated every 6 months for HCC periodic screening for at least 1 year. None of the selected patients in this subgroup developed liver tumor during this time.
2. Small HCC group: patients with cirrhosis and small HCC within the Milan criteria (13; single tumor <5 cm or 3 nodules <3 cm) and eligible for curative treatment; all these patients underwent radiofrequency ablation (RFA) by the same operator during which a percutaneous biopsy for histologic assessment of HCC was conducted before ablation. Only patients with biopsy-proven HCC were selected in this subset. All of them were then followed-up using abdominal computed tomography (CT) scan, serum AFP assessment, and physical examination at 1 month then every 3 months. Patients with partial response at 1 month defined by a persistent enhancement of the lesion on CT scan could have been retreated by RFA. Follow-up ended at the date of death or liver transplantation, or at the last recorded visit (or information) within the last 6 months before December 2011. Overall survival was defined by the time between the day of inclusion and death, liver transplantation, or last visit recorded until December 2011. Recurrence-free survival was defined by the time between the date of inclusion and the date of HCC recurrence.
3. Large HCC group: patients with cirrhosis and large HCC outside the Milan criteria (multinodular HCC and/or tumoral portal vein thrombosis and/or extrahepatic metastases; ref. 1) with these patients being eligible for palliative treatment.

Published OnlineFirst November 7, 2012; DOI: 10.1158/1078-0432.CCR-12-1099

^{1}H NMR spectroscopy

For NMR analysis, samples were thawed at room temperature. A volume of 0.6 mL of serum was placed into a 5-mm diameter-specific tube together with 0.1 mL of D_2O containing a known amount of fumaric acid (6.5 mg/mL). The deuterium oxide was used for the spectrometer locking and fumaric signal for chemical shift calibration at 6.53 parts per million (ppm). The addition of this acid solution lowered the sera pH of 0.1 units (identical for all samples). The resulting pH samples were between 8.4 and 8.7. Fumaric acid as an internal reference presents the advantages to produce a single signal located in a spectral region without other interfering resonances. The proton spectra were acquired at 500 MHz on a Varian Unity Inova spectrometer at 298 K. A signal was acquired after a 90° pulse of 32 K data points on a spectral window of 5,000 Hz. The relaxation delay was 4 seconds. The water signal was suppressed by a presaturation sequence using low-power irradiation (0.03 W for 2 seconds) on the water-signal frequency during the relaxation delay. Frequently, the CPMG sequence is used to suppress the broad signal of protein according to their short relaxation time. Because the lipid changes in the serum of patients with HCC, we have used a single pulse sequence to preserve the complete lipid profile of our spectra. The resulting free induction decays obtained with 128 transients were processed by Mestrec software. A Fourier transformation was applied with an exponential window function to produce a 1-Hz broadening line. Spectra were phased and a spline baseline correction was applied with 3 points at 0.5 and 9 ppm. The spectral region between 0 and 9 ppm was divided into 9,000 spectral regions of 0.001 ppm width, called buckets, using a personal program with R. Water, urea (signal damaged by water-saturation transfer), and fumaric-acid regions were excluded (1,810 variables excluded). Each bucket was integrated and scaled to the total summed integrals for each spectrum.

For resonance assignment purpose, ^{1}H–^{1}H total correlation spectroscopy (TOCSY) 2D NMR spectra were also acquired at 298 K for some samples with a mixing time of 80 milliseconds, 4,000 data points and 32 transients for each of the 512 increments.

Univariate statistical analyses

Qualitative variables were compared using Fisher exact test, the χ^2 test, or the χ^2 trend test with 1 degree of freedom. Quantitative variables were compared using the nonparametric Wilcoxon test. All reported P values are 2-tailed. Associations were considered statistically significant at a 2-tailed α of 0.05.

Multivariate statistical analyses

A principal component analysis (PCA) was first conducted to detect any outliers or group separation based on NMR signal variability.

An orthogonal projection to latent structure (OPLS) analysis was run to discriminate patients from the cirrhosis or large HCC groups. Compared with the classical projection of latent-structure analysis (PLS), this method allowed improved interpretation of the spectroscopic variations between discriminated groups, by removing information that had no impact on discrimination.

Samples were split into 3 sets: training set, test set, and small HCC set. The training set was used to build the OPLS model. The test set was projected on the OPLS model for validation and to assess the general predictive power of the model.

The training and test sets were randomly constituted of 84 training cases (62 cirrhosis and 22 large HCC) and 42 test cases (31 cirrhosis and 11 large HCC). The small HCC set included 28 small HCC cases and the same 31 cirrhosis cases used in the test set.

The goodness-of-fit parameters of the OPLS model, R^2X, R^2Y, and Q^2Y, were calculated. R^2X and R^2Y represent the explained variance, respectively, of the X and the Y matrices. Q^2Y estimates the predictability of the model. $R^2 = 1$ indicates a perfect description of the data by the model, whereas $Q^2 = 1$ indicates perfect predictability. For internal validation of the OPLS models, we conducted a permutation test (999 permutations). The aim of this test was to evaluate whether our OPLS models, built with the groups, was significantly better than any other OPLS model obtained by randomly permuting the original groups attribution.

For validation, a receiver–operator characteristic (ROC) curve was drawn to evaluate the ability of the OPLS latent variable T_{pred} to correctly classify the test set. The area under the ROC (AUROC) was calculated. A perfect discrimination corresponded to an AUROC equal to 1. An optimal cutoff value of T_{pred} (T_{opt}) was also calculated with the Matlab function "perfcurve," which minimize both the false-positive and false-negative cases in the test set, assuming equal weightings on the cost of misclassification.

The small HCC set was used to test the ability of the model to discriminate between small HCC observations and cirrhosis cases. False-positive and false-negative rates were calculated using the curve cutoff, T_{opt}, previously calculated for the test set.

A score plot illustrated the results. Each point in the score plot represented the projection of an NMR spectrum (and thus a patient's sample) on the predictive (horizontal axis) and the first orthogonal component of the model (vertical axis).

The loading plot represents the covariance between the Y-response matrix and the signal intensity of the various spectral domains. Colors were also used in the loading plot depending of the P value associated with the correlation between the corresponding bucket intensity and the Y variable. The null hypothesis associated with the P values used in this study is that there is no correlation between X (intensity of the buckets) and Y (cirrhotic group or HCC group) variables. To minimize false-positive rates in multiple comparisons of the 4,239 spectral domains, we used the conservative Bonferroni correction, which discards any low significant variables. Thus, for an error rate of 0.01, a metabolite variation in the loading plot was considered significant if its P value was less than 2.4×10^{-6}.

Published OnlineFirst November 7, 2012; DOI: 10.1158/1078-0432.CCR-12-1099

PCA and OPLS analyses were conducted using Simca-P12 (Umetrics) and in-house Matlab (Mathworks) code based on Trygg and Wold method (14).

Metabolite identification

On the loading plot, the positive signals corresponded to those metabolites that had an increased concentration in the serum of patients with HCC. Conversely, a negative signal corresponded to those metabolites that had an increased concentration in the serum of patients without HCC.

The buckets were designated according to their central chemical-shift values. Their most probable assignment to a metabolite was given according to the spectral assignment, as previously described in the literature (15), and was confirmed with ^{1}H–^{1}H TOCSY 2D NMR spectra.

Results

Patients′ characteristics

A total of 286 patients were screened: of these, 158 patients fulfilled the inclusion criteria as shown in Fig. 1. The data obtained by bucketing of the 158 serum spectra were successfully acquired and first analyzed by PCA (results not shown). From this analysis, 4 outliers were identified. All spectra that exhibited high levels of ethanol (1.11 and 3.66 ppm) were excluded. Demographics, clinical, and biologic features, as well as data about characteristics of liver tumors for the 154 remaining patients, are displayed in Table 1. As expected, patients with HCC were older and were more often male than patients without HCC. There was no difference in the severity of liver disease as assessed by the Model for End-Stage Liver Disease (MELD) score between the 3 groups.

OPLS model with cirrhosis and large HCC

Serum spectra from cirrhotic and large HCC groups that belonged to the training set were discriminated with the OPLS model as shown in the score plot in Fig. 2A. The model was build with 1 predictive and 3 Y-orthogonal components and exhibited a good explained variance: (R^2X) of 0.46, (R^2Y) of 0.90, predictability (Q^2Y) of 0.83.

The model was internally validated, as all Q^2Y and R^2Y values obtained with permuted Y were smaller than those of the model. Intercept values for Q^2Y and R^2Y obtained from the permutation plot (not shown) were, respectively, −0.57 and 1.40.

Validation conducted with the test set shows that the model could predict cirrhosis or HCC as shown in the score plot in Fig. 3A. In all cases, each sample was correctly classified according to the presence or absence of large HCC. Consequently, the AUROC was equal to 1 (not shown). The optimal cutoff value of T_{pred} was $T_{opt} = 0.25$.

Small HCC set

As shown in the score plot in Fig. 3B the projection of cirrhotic and small HCC on the predictive component was heterogeneous.

Using the optimal cutoff value of T_{pred} obtained from the test set ($T_{opt} = 0.25$), all cirrhotic sera were correctly assigned to the cirrhotic groups but, among the 28 small

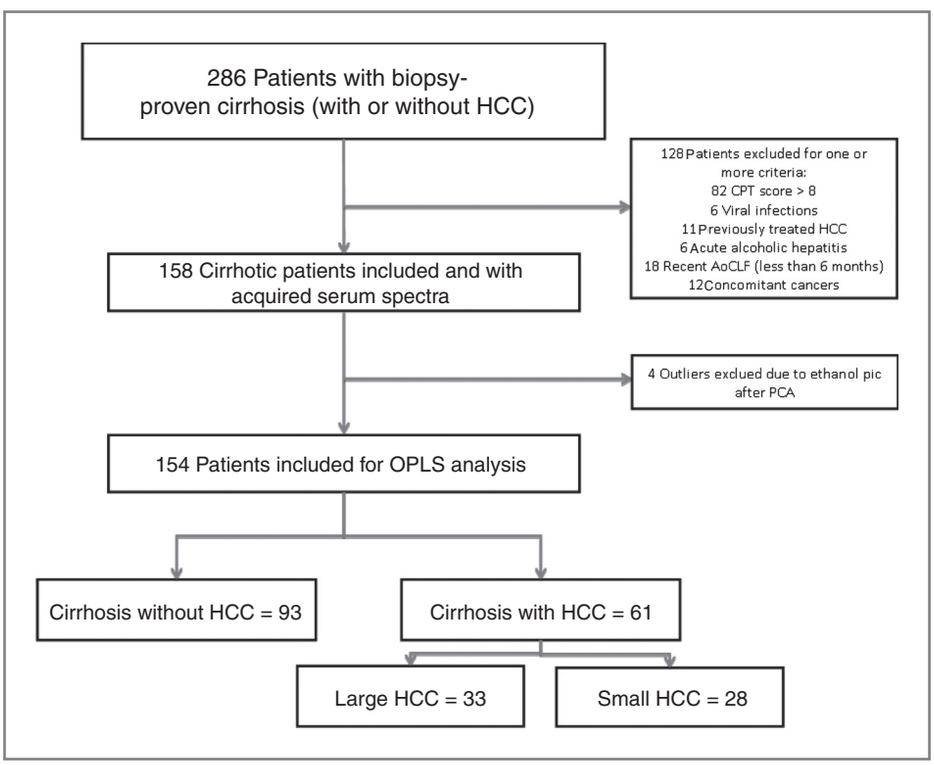

Figure 1. Flow chart of patients. CPT, Child–Pugh–Turcott score; AoCLF, acute on chronic liver failure.

Published OnlineFirst November 7, 2012; DOI: 10.1158/1078-0432.CCR-12-1099

Table 1. Baseline characteristics of the population

	Training set ($n = 84$)		Test set ($n = 42$)		Small HCC projections ($n = 28$)
	Cirrhosis ($n = 62$)	Large HCC ($n = 22$)	Cirrhosis ($n = 31$)	Large HCC ($n = 11$)	
Age, y[a]	59.0 ± 1.4	71.7 ± 1.7[c]	59.5 ± 2.2	66.3 ± 2.5	66.7 ± 1.3[c]
Male gender[b]	53 (85%)	22 (100%)[c]	27 (81%)	11 (100%)	22 (28%)
ALT (UI/L)[a]	41.1 ± 2.5	53 ± 11.4	47.0 ± 7.8	38.5 ± 7.2	49.5 ± 12.2
AST (UI/L)[a]	75.9 ± 6.8	97.3 ± 26.7	72.4 ± 12.4	54.5 ± 5.9	62.0 ± 7.5
Albumin (g/L)[a]	38.9 ± 0.7	37.3 ± 1.0	37.9 ± 1.2	37.7 ± 1.5	39.8 ± 1.0
Prothrombin level (% control)[a]	72.5 ± 2.2	75.4 ± 3.7	70.0 ± 3.5	69.1 ± 4.7	69.9 ± 2.7
Bilirubin (μmol/L)[a]	23.6 ± 3.3	17.9 ± 2.1	29.4 ± 4.1	26.6 ± 8.7	17.1 ± 1.7
Child–Pugh score[a]	5.8 ± 0.1	6.0 ± 0.2	6.3 ± 0.2	6.2 ± 0.3	5.5 ± 0.2[c]
MELD score[a]	11.3 ± 0.5	11.1 ± 1.0	11.9 ± 0.8	13.4 ± 2.1	10.5 ± 0.8
Creatinine, μmol/L[a]	87.0 ± 4.8	101.3 ± 8.6	79.2 ± 3.1	136.1 ± 40.5[c]	82.2 ± 5.5
Blood glucose, mmol/L	6.3 ± 0.3	6.1 ± 0.3	8.0 ± 0.9	7.0 ± 0.9	6.3 ± 0.4
Triglyceride, g/L[a]	1.1 ± 0.1	1.5 ± 0.3	1.5 ± 0.2	1.2 ± 0.1	1.1 ± 0.1
Total cholesterol, mmol/L[a]	4.4 ± 0.2	4.9 ± 0.6	4.6 ± 0.3	5.0 ± 0.6	4.8 ± 0.3
AFP, ng/mL[a]	10.3 ± 3.1	6,156.2 ± 3,947.6[c]	18.0 ± 4.0	5,665.2 ± 5,484.3	179.4 ± 178.3[d]
HCC characteristics					
Number of nodules	—	2.4 ± 0.3	—	3.6 ± 0.8	1.2 ± 0.1[d]
Size (mean sum of nodules, mm)	—	93.1 ± 9.4	—	100.1 ± 12.2	31.9 ± 2.9[d]
PVT (number, %)	1 (2%)	8 (36%)	—	2 (18%)	0 (0%)
Metastasis (number, %)	—	3 (14%)	—	1 (9%)	0 (0%)

NOTE: All biologic and clinical parameters were recorded at inclusion.

Abbreviations: ALT, alanine aminotransferase; AST, aspartate aminotransferase; PVT, portal vein thrombosis.

[a]Mean ± SEM.

[b]Number (percentage) of patients.

[c]$P < 0.05$ between HCC and cirrhosis.

[d]$P < 0.05$ between large and small HCC groups.

HCC group, 11 patients displayed a serum metabolic profile similar to that of patients with large HCC (true positive), whereas 17 had a metabolic profile close to that observed in cirrhotic patients without HCC (false negative).

Having identified 2 different metabolomic profiles in this subset of patients, we compared their baseline features as well as their outcomes after the RFA procedure (Table 2). If their clinical and radiologic characteristics were comparable, there was a nonsignificant trend toward higher rates of local or distant recurrence, as well as a higher rate of deaths during follow-up in patients with serum metabolomic profiles defining the true-positive subset.

Discriminant metabolites

The appearance of ^{1}H NMR serum spectra was globally similar to those previously described in human sera of cirrhotic patients (Supplementary Fig. S1; ref. 11). The spectral assignment was confirmed with ^{1}H–^{1}H TOCSY 2D NMR spectra (Supplementary Fig. S2).

The loading plot obtained with the OPLS model for the training set revealed that 12 signals, corresponding to 8 metabolites or groups of metabolites, were highly significantly correlated with the presence of large HCC (Fig. 2B). They are presented in Table 3.

In ^{1}H NMR serum spectra, lipids could be detected as broad resonances of fatty-acid methyl and methylene moieties at 0.8 and 1.24 ppm, respectively, and the N-trimethyl moiety of choline was included in phospholipids at 3.22 ppm as shown in Fig. 1. Among those signals, those at 0.8 and 1.24 ppm were significantly correlated to the presence of large HCC. These resonances of fatty acids arise from lipids included lipoprotein particles of different densities. It has been widely reported that high-density lipid (HDL) particles produce resonances with lower chemical shifts than low-density lipoprotein [LDL and very low-density lipoprotein (VLDL)] particles. Interestingly, lipoproteins with higher density were significantly elevated in cirrhotic patients without HCC. For VLDL, corresponding to the highest chemical shifts in methyl and methylene resonances, no differences were found. Others lipids were identified and participated in the discrimination.

Three other broad lipid signals were identified in the patients' sera at 1.50, 1.99, and 5.33 ppm. The 2 first corresponded to methylene moieties following the ester moiety. The last one corresponded to methylene moiety following a double bound in unsaturated fatty acid.

N-acetyl moieties of glycoprotein produced a broad resonance at 2.05 ppm, which was increased for patients with

Published OnlineFirst November 7, 2012; DOI: 10.1158/1078-0432.CCR-12-1099

HCC when compared with those without HCC. This signal corresponded to different N-acetylated glycoproteins as well as to their metabolites: N-acetylneuraminic acid and N-acetylglucosamine.

Some amino acids were identified in the spectra and were highly significant for discrimination. Glutamine was significantly higher in cirrhotic patients than patients with HCC, whereas glutamate was significantly lower.

Ketone bodies could be detected in the spectra and participated in discrimination. Acetate (1.92 ppm) was significantly higher in HCC than cirrhotic patients.

Discussion

This preliminary study was conducted in a homogeneous and large sample-sized cohort of patients. The usual major limitation encountered in a translational metabolomic approach to liver diseases is methodologic bias when selecting patients, thus limiting the confidence that can be drawn from conclusions (8, 9, 16). We attempted to avoid these pitfalls by constructing well-defined subgroups of patients according to their stage of underlying liver disease and HCC status. We also focused specifically on alcoholic etiology to avoid any potential specific influence of viral or nonalcoholic-related liver disease on sera metabolomic profiles, as previously reported (17, 18). Moreover, to eliminate the effect of liver-function impairment on different metabolic pathways (as previously reported), we excluded all patients with end-stage liver disease from this analysis (11). Also, the collection of sera samples before the onset of any therapeutic procedure for HCC reinforced the confidence of the observed effect of tumor metabolism.

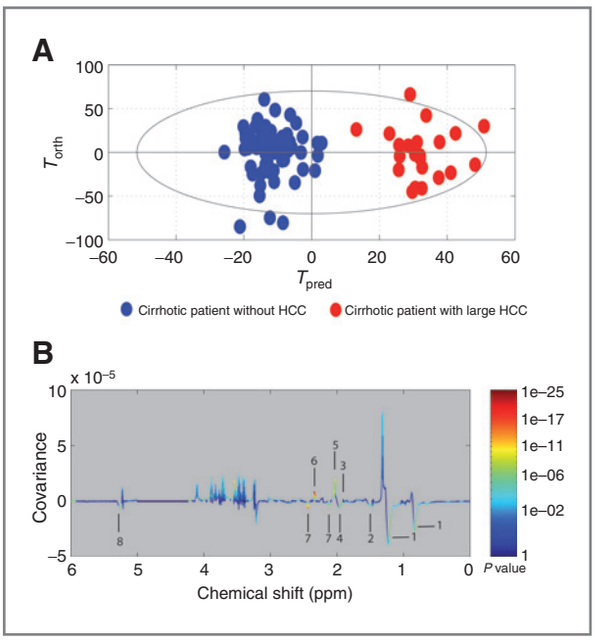

Figure 2. OPLS score plot (A) and loading plot (B). A, on the score plot, each dot corresponds to a spectrum colored according to the absence (blue) or the presence (red) of HCC. The constructed model displays a good separation between the spectrum of cirrhotic patients without HCC and those with HCC. B, on the loading plot, variations of bucket intensities are represented using a line plot between 0 and 6 ppm. Positive signals correspond to the metabolites present at increased concentrations in patients with large HCC. Conversely, negative signals correspond to the metabolites present at increased concentrations in patients without HCC. The buckets are labeled according to the metabolite as presented in Table 2.

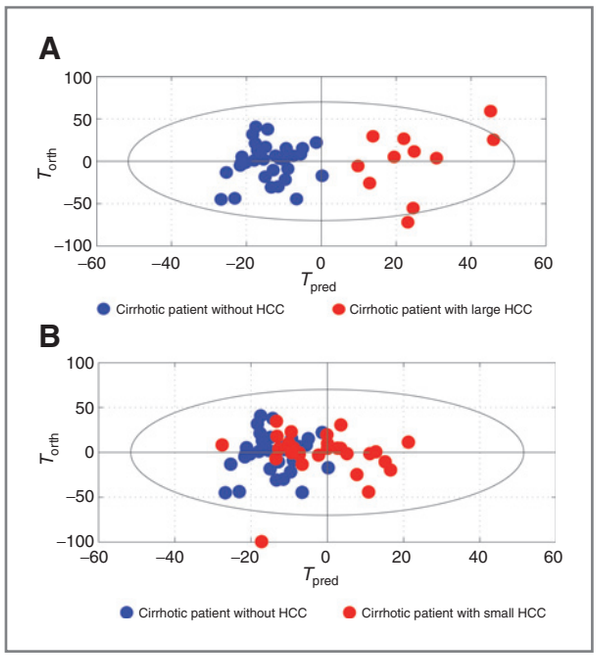

Figure 3. Validation of the model (A) and projection of serum spectra in patients from the cirrhosis or small HCC group (B). Each dot corresponds to a spectrum colored depending on the absence (blue) or presence (red) of HCC. A, each new spectrum was projected in the score plot using the previously constructed model to enable prediction of the presence or absence of HCC. The AUROC characteristic was drawn to evaluate the ability of the orthogonal projection to latent structure (OPLS) analysis latent variable. T_{pred}, to correctly classify each spectrum was equal to 1 with a cutoff of T_{pred} (T_{opt}) equal to 0.25. B, using the same previously calculated cutoff value of the training set ($T_{opt} = 0.25$), each spectrum of cirrhotic patients without HCC was correctly assigned. Nevertheless, the spectra from patients with small HCC had a heterogeneous distribution in the score plot. Some were projected on the left with the cirrhotic spectra, others were projected on the right with the patients with large HCC and some were projected in between.

In this setting, the present data enabled us to draw several conclusions. First, it seems that changes in serum metabolomic profiles were observed according to the presence of advanced HCC. Second, these fingerprints reflected the distinct activation or impairment of multiple biologic pathways, mainly energetic metabolism involving glutamine/glutamate, ketone bodies, and lipids. On another hand, glucose sera content was not a discriminant metabolite. Finally, the refinement of our initial projection, to analyze metabolic changes observed in patients with biopsy-proven small HCC, revealed various profiles that probably reflect different metabolic activities with potential clinical implications.

The metabolic profiles of cirrhotic patients with large HCC exhibited clear modifications in lipid composition,

Published OnlineFirst November 7, 2012; DOI: 10.1158/1078-0432.CCR-12-1099

Table 2. Characteristics of small HCC according to their projection on the model

	False negative[c] ($n = 17$)	True positive[d] ($n = 11$)
Age, y[a]	64.8 ± 1.7	69.9 ± 1.8
Male gender[b]	12/17	10/11
Child	5.2 ± 0.1	6.1 ± 0.3
MELD	9.9 ± 0.5	11.5 ± 1.2
Number of tumors	1.3 ± 0.1	1.2 ± 0.1
Size of tumors (mm)	33.2 ± 4.5	30.1 ± 3.1
Edmondson grade (1/2/3)	3/11/3	2/7/2
Liver glutamine synthase[e]	38%	25%
Recurrence[b]	7 (41%)	7 (63%)
Overall mortality[b]	4 (23%)	6 (54%)

[a]Mean ± SEM.
[b]Number (percentage) of patients.
[c]False negative corresponds to proven-biopsy HCC case projected with the cirrhosis cases.
[d]True positive corresponds to proven-biopsy HCC case projected with large HCC cases.
[e]Glutamine synthase was considered positive when more than 50% of tumor cells showed a strong cytoplasmic staining. Results were expressed in percentage of positive biopsy.

glutamine metabolism, and ketone bodies as compared with the metabolic profiles obtained from cirrhotic patients without HCC as previously described using mass spectroscopy or ^{1}H NMR spectroscopy in urine, tissue, or serum (7–10, 16, 19, 20). However, those metabolic profiles were mainly described with viral etiology and not in alcoholic cirrhotic patients with well-classified HCC.

Patients with advanced HCC had lower HDL than cirrhotic patients without HCC. Using serum ^{1}H NMR spectroscopy of cirrhotic patients, we have previously confirmed that HDL level is altered and decreased with the severity of chronic liver failure (11). Patients with end-stage liver disease were excluded, thus, differences in HDL could not be explained by the severity of liver disease. Interestingly, several epidemiologic studies have reported a good correlation between with low HDL-cholesterol levels and several cancers, including HCC (21). In the population studied here, cholesterolemia was not modifying in the presence of HCC (Table 1). Nevertheless, the lipoprotein profile, as assessed with NMR spectra, showed that HDL fraction (not HDL-cholesterol) could be modulated in sera of patients with HCC. However, low HDL levels may be a nonspecific surrogate marker for an existing malignancy rather than a predisposing factor. Unsaturated lipids were also found at higher levels in patients without cancer.

Glutaminolysis and glycolysis represent the main metabolic energy pathways in cell tumors. Alterations in glutamine metabolism in this context may have several explanations. First, "trapping" of glutamine by malignant cells could explain the glutamine depletion in the serum of HCC patients when compared with the cirrhotic patients in our study. Yang and colleagues showed, using high resolution magic angle spinning spectroscopy, in simultaneous samples of HCC and non-HCC tissues obtained from the same patients, elevated levels of glutamine in tumor samples: the levels were higher in high-grade tumors than low-grade or nontumoral tissues (20). Glutamine consumption by tumor cells has been reported and seems to depend upon the presence or absence of an alternative energy substrate (22). Moreover, low levels of glutamine and high levels of glutamate in serum may be found in different states as cachexia, cancer (specifically digestive cancers) or proinflammatory states. In these clinical settings, high glutamate levels were secondary to the accumulation of this metabolite in the serum in parallel with a decrease in muscular glutamate intake (23).

The role of glycoproteins in cancer disease has been widely studied. Using data from ^{1}H NMR spectroscopy of

Table 3. Discriminant metabolites observed by ^{1}H NMR spectroscopy, according to the loading plot (Fig. 2B), between cirrhotic serum spectra and large HCC serum spectra

Number	Name	Chemical shift (ppm) and multiplicity	*r*	*P*
1	Methyl moieties of fatty acids (HDL)	0.84^{m} 1.23^{m}	−0.60	5.22×10^{-9}
2	Methylene moieties of fatty acids	1.50^{m}	−0.56	4.09×10^{-6}
3	Acetate	1.90^{s}	+0.57	2.56×10^{-8}
4	Methylene moieties of fatty acids (β of esters)	1.99^{b}	−0.48	5.42×10^{-6}
5	N-acetyl moiety	2.02^{m}	+0.52	5.68×10^{-7}
6	Glutamate	2.33^{m}	+0.83	1.23×10^{-21}
7	Glutamine	2.11^{m} 2.43^{m}	−0.63	3.92×10^{-12}
8	Fatty acids double bounds	5.33^{b}	−0.42	6.50×10^{-7}

NOTE: The metabolite number corresponds to the label in the loading plot in Fig. 2B. Chemical shift (referenced to fumaric acid signal at 6.53 ppm) and multiplicity correspond to those found in the ^{1}H NMR spectra of the patient's serum at 298 K. ^{s}, singlet; ^{d}, doublet; ^{dd}, doublet of doublet; ^{t}, triplet; ^{m}, multiplet; ^{b}, broadsignal. A negative correlation (*r*) corresponds of an increased metabolite concentration in the cirrhotic group and a positive correlation to an increased metabolite concentration in the HCC group.

Published OnlineFirst November 7, 2012; DOI: 10.1158/1078-0432.CCR-12-1099

serum or plasma, the prominent resonance in the region of 2.0 to 2.1 ppm has been frequently associated with tumor invasion or malignancy in several types of cancer, including colorectal, gastric, breast, cervical, prostate, and ovarian (6). Nicholson and colleagues have suggested that this resonance arises mainly from N-acetyl protons from α1 acid glycoprotein. This glycoprotein contains a high ratio of carbohydrate (45%), as N-linked glycans of a sialic-acid type (15). More specifically, in HCC, raised levels of α1 acid glycoprotein had been found in patients with cancer, as well as low AFP, when compared with cirrhotic patients without cancer (24).

Thus, serum metabolomic analysis of cirrhotic patients with large HCC highlights the activation of various metabolic pathways that seem to be specific to this tumor. On the basis of the present data, metabolomic NMR analysis provides new insights into the metabolic processes related to the biology of liver cancer. Furthermore, the projection of small HCC serum samples along predefined discriminant axes reveals important clinical information. Indeed, based on the serum analysis of these "intermediate" patients, we were able to observe a subgroup of patients whose metabolomic profiles were similar to those of patients with large HCC, whereas other "intermediate" patients displayed fingerprints suggesting an absence of liver cancer.

The model failed to clearly discriminate between cirrhotic patients and small HCC patients. However, from a metabolomic point of view, some patients with small HCC, who were eligible for curative treatment, seemed to behave as patients with advanced cancerous disease.

HCC recurrence after curative treatment (whether RFA, surgical resection, or transplantation) is a major challenge as tumor recurrence can be as high as 50% at 2 years (1). Thus, we attempted to classify patients with small HCC according to their serum metabolomic profile and compared HCC characteristics within this subgroup (Table 2). We did not observe any differences according to clinical characteristics or HCC status (number, size, histologic features comprising expression of glutamine synthase): this suggests a certain degree of homogeneity that does not account for the identified metabolomic changes. However, there was a trend toward a worse prognosis in patients with profiles similar to the large HCC group, with higher rates of local or distant recurrences and a greater incidence of death, although these findings must be cautiously interpreted because of the small sample-size of this subpopulation (25). By providing new patterns of recognition, metabolomic profiling may be a useful tool to refine prognosis and to aid therapeutic procedures for these patients.

However, metabolomic profiling, which assesses surrogate markers of tumor biology in tumoral tissues or serum samples, can provide complete and multivariate information on metabolomic changes related to liver tumors and can possibly assess its aggressiveness, thus defining various metabolic profiles. The assessment of this technique as a prognosis tool in patients with HCC and who are eligible for curative treatment deserves further investigation, particularly in HCV- or HBV-infected patients with HCC in whom metabolomic changes reported here may not be entirely translated. Most importantly, the intraindividual analysis of serum changes during follow-up of treated patients may provide essential information related to therapeutic responses, recurrence, or progression. These new approaches should be developed in large prospective cohorts of well-defined patients undergoing standardized therapeutic procedures classified according to both the etiology on the underlying liver disease and the stage of liver tumor, and in whom sequential biologic samples are available for metabolomic profiling. Finally, the additional integration of metabolomic information, which may improve the performance of preexisting risk-assessment models for HCC occurrence or recurrence after treatment, warrants to be tested in large cohorts of prospective followed-up patients with cirrhosis. Such approach will surely improve our understanding of the implications of the various biologic pathways involved in the progression toward cancer diseases and may, in the near future, help identify subgroups of patients at high risk of HCC, and so could benefit from specific preventive measures or could be given adapted screening policies.

Disclosure of Potential Conflicts of Interest

No potential conflicts of interest were disclosed.

Authors' Contributions

Conception and design: P. Nahon, R. Amathieu, O. Seror, J.-C. Trinchet, M. Beaugrand, L. Le Moyec

Development of methodology: P. Nahon, R. Amathieu, M.N. Triba, L. Le Moyec

Acquisition of data (provided animals, acquired and managed patients, provided facilities, etc.): P. Nahon, R. Amathieu, N. Bouchemal, J.-C. Nault, M. Ziol, O. Seror

Analysis and interpretation of data (e.g., statistical analysis, biostatistics, computational analysis): P. Nahon, R. Amathieu, M.N. Triba, J.-C. Nault, O. Seror, G. Dhonneur, J.-C. Trinchet, M. Beaugrand, L. Le Moyec

Writing, review, and/or revision of the manuscript: P. Nahon, R. Amathieu, M.N. Triba, O. Seror, G. Dhonneur, M. Beaugrand, L. Le Moyec

Administrative, technical, or material support (i.e., reporting or organizing data, constructing databases): P. Nahon, R. Amathieu, M.N. Triba, O. Seror

Study supervision: P. Nahon, R. Amathieu, L. Le Moyec

Grant Support

This work was supported by grants from Paris 13 University.

The costs of publication of this article were defrayed in part by the payment of page charges. This article must therefore be hereby marked *advertisement* in accordance with 18 U.S.C. Section 1734 solely to indicate this fact.

Received April 7, 2012; revised September 10, 2012; accepted October 10, 2012; published OnlineFirst November 7, 2012.

References

1. Llovet JM, Bruix J. Novel advancements in the management of hepatocellular carcinoma in 2008. J Hepatol 2008;48(Suppl 1):S20–37.

2. Breuhahn K, Gores G, Schirmacher P. Strategies for hepatocellular carcinoma therapy and diagnostics: lessons learned from high

Published OnlineFirst November 7, 2012; DOI: 10.1158/1078-0432.CCR-12-1099

throughput and profiling approaches. Hepatology 2011;53: 2112–21.
3. Lindon JC, Nicholson JK. Spectroscopic and statistical techniques for information recovery in metabonomics and metabolomics. Annu Rev Anal Chem (Palo Alto Calif) 2008;1:45–69.
4. Nicholson JK, Lindon JC, Holmes E. 'Metabonomics': understanding the metabolic responses of living systems to pathophysiological stimuli via multivariate statistical analysis of biological NMR spectroscopic data. Xenobiotica 1999;29:1181–9.
5. Slupsky CM, Steed H, Wells TH, Dabbs K, Schepansky A, Capstick V, et al. Urine metabolite analysis offers potential early diagnosis of ovarian and breast cancers. Clin Cancer Res 2010;16:5835–41.
6. Spratlin JL, Serkova NJ, Eckhardt SG. Clinical applications of metabolomics in oncology: a review. Clin Cancer Res 2009;15:431–40.
7. Chen T, Xie G, Wang X, Fan J, Qiu Y, Zheng X, et al. Serum and urine metabolite profiling reveals potential biomarkers of human hepatocellular carcinoma.Mol Cell Proteomics 2011;10:M110.004945.
8. Gao H, Lu Q, Liu X, Cong H, Zhao L, Wang H, et al. Application of ^{1}H NMR-based metabonomics in the study of metabolic profiling of human hepatocellular carcinoma and liver cirrhosis. Cancer Sci 2009;100:782–5.
9. Shariff MI, Gomaa AI, Cox IJ, Patel M, Williams HR, Crossey MM, et al. Urinary metabolic biomarkers of hepatocellular carcinoma in an Egyptian population: a validation study. J Proteome Res 2011;10:1828–36.
10. Wu H, Xue R, Dong L, Liu T, Deng C, Zeng H, et al. Metabolomic profiling of human urine in hepatocellular carcinoma patients using gas chromatography/mass spectrometry. Anal Chim Acta 2009;648: 98–104.
11. Amathieu R, Nahon P, Triba M, Bouchemal N, Trinchet JC, Beaugrand M, et al. Metabolomic approach by ^{1}H NMR spectroscopy of serum for the assessment of chronic liver failure in patients with cirrhosis. J Proteome Res 2011;10:3239–45.
12. Bruix J, Sherman M, Llovet JM, Beaugrand M, Lencioni R, Burroughs AK, et al. Clinical management of hepatocellular carcinoma. Conclusions of the Barcelona-2000 EASL conference. European Association for the Study of the Liver. J Hepatol 2001;35:421–30.
13. Mazzaferro V, Regalia E, Doci R, Andreola S, Pulvirenti A, Bozzetti F, et al. Liver transplantation for the treatment of small hepatocellular carcinomas in patients with cirrhosis. N Engl J Med 1996;334:693–9.
14. Trygg J, Wold S. Orthogonal projections to latent structures (O-PLS). J Chemometrics 2002;16:116–28.
15. Nicholson JK, Foxall PJ, Spraul M, Farrant RD, Lindon JC. 750 MHz ^{1}H and ^{1}H-^{13}C NMR spectroscopy of human blood plasma. Anal Chem 1995;67:793–811.
16. Shariff MI, Ladep NG, Cox IJ, Williams HR, Okeke E, Malu A, et al. Characterization of urinary biomarkers of hepatocellular carcinoma using magnetic resonance spectroscopy in a Nigerian population. J Proteome Res 2010;9:1096–103.
17. Cobbold JF, Patel JH, Goldin RD, North BV, Crossey MM, Fitzpatrick J, et al. Hepatic lipid profiling in chronic hepatitis C: an *in vitro* and *in vivo* proton magnetic resonance spectroscopy study. J Hepatol 2008;52: 16–24.
18. Puri P, Wiest MM, Cheung O, Mirshahi F, Sargeant C, Min HK, et al. The plasma lipidomic signature of nonalcoholicsteatohepatitis. Hepatology 2009;50:1827–38.
19. Patterson AD, Maurhofer O, Beyoglu D, Lanz C, Krausz KW, Pabst T, et al. Aberrant lipid metabolism in hepatocellular carcinoma revealed by plasma metabolomics and lipid profiling. Cancer Res 2011;71: 6590–600.
20. Yang Y, Li C, Nie X, Feng X, Chen W, Yue Y, et al. Metabonomic studies of human hepatocellular carcinoma using high-resolution magic-angle spinning ^{1}H NMR spectroscopy in conjunction with multivariate data analysis. J Proteome Res 2007;6:2605–14.
21. Ahn J, Lim U, Weinstein SJ, Schatzkin A, Hayes RB, Virtamo J, et al. Prediagnostic total and high-density lipoprotein cholesterol and risk of cancer. Cancer Epidemiol Biomarkers Prev 2009;18: 2814–21.
22. Meng M, Chen S, Lao T, Liang D, Sang N. Nitrogen anabolism underlies the importance of glutaminolysis in proliferating cells. Cell Cycle 2010;9:3921–32.
23. Hack V, Stutz O, Kinscherf R, Schykowski M, Kellerer M, Holm E, et al. Elevated venous glutamate levels in (pre)catabolic conditions result at least partly from a decreased glutamate transport activity. J Mol Med (Berl) 1996;74:337–43.
24. Bachtiar I, Kheng V, Wibowo GA, Gani RA, Hasan I, Sanityoso A, et al. Alpha-1-acid glycoprotein as potential biomarker for alpha-fetoprotein-low hepatocellular carcinoma. BMC Res Notes 2010; 3:319.
25. Di Tommaso L, Destro A, Seok JY, Balladore E, Terracciano L, Sangiovanni A, et al. The application of markers (HSP70 GPC3 and GS) in liver biopsies is useful for detection of hepatocellular carcinoma. J Hepatol 2009;50:746–54.

AACR American Association for Cancer Research

Clinical Cancer Research

Identification of Serum Proton NMR Metabolomic Fingerprints Associated with Hepatocellular Carcinoma in Patients with Alcoholic Cirrhosis

Pierre Nahon, Roland Amathieu, Mohamed N. Triba, et al.

Clin Cancer Res 2012;18:6714-6722. Published OnlineFirst November 7, 2012.